Tellus (2005), 57B, 58–69
Printed in UK. All rights reserved

TELLUS

Variations and trends of CO_2 in the surface seawater in the Southern Ocean south of Australia between 1969 and 2002

By HISAYUKI YOSHIKAWA-INOUE[1]* and M. ISHII[2], [1]*Laboratory of Marine and Atmospheric Geochemistry, Graduate School of Environmental Earth Sciences, Hokkaido University, Kita-10, Nishi-5, Kita-ku, Sapporo 060-0810, Japan;* [2]*Department of Geochemistry, Meteorological Research Institute, Nagamine 1-1, Tsukuba, Ibaraki 305-0052, Japan*

(Manuscript received 16 September 2003; in final form 6 July 2004)

ABSTRACT

Measurements of the partial pressure of CO_2 in surface seawater (pCO_2^{sw}) were made in the Southern Ocean south of Australia during four cruises in January to February 1969, December 1983 to January 1984, December 1994 to January 1995 and January 2002. The spatial distribution of pCO_2^{sw} for the four cruises showed the same pattern north of the Sub-Antarctic Front (SAF), while year-to-year changes were noted south of the SAF. We evaluated the long-term trend of the pCO_2^{sw} representative of the zone between oceanographic fronts by taking into account changes in the seasonal variation in pCO_2^{sw} and the long-term increase of the sea-surface temperature (SST) of the Southern Hemisphere. The observed growth rate of pCO_2^{sw} was 0.7 ± 0.1 μatm yr^{-1} at its minimum, which was observed at the SST of 15 °C north of the Subtropical Front (STF), 1.0 ± 0.5 μatm yr^{-1} in the Sub-Antarctic Zone (SAZ) between STF and SAF, 1.5 ± 0.4 μatm yr^{-1} in the Polar Frontal Zone (PFZ) between SAF and the Polar Front (PF) and 1.8 ± 0.2 μatm yr^{-1} in the Polar Zone (PZ) between PF and 62°S, determined as the northern edge of the Seasonal Sea Ice Zone (SSIZ) on the basis of surface salinity and satellite images. These increases were caused by the uptake of anthropogenic CO_2 as well as variations in the thermodynamic temperature effect, ocean transport and biological activity. In the SSIZ between 62 and 66.5°S, we could not clearly evaluate the long-term trend of pCO_2^{sw} due to the remarkable CO_2 drawdown due to biological activity in January 2002. The relatively low growth rates of pCO_2^{sw} close to the STF and in the SAZ are probably associated with the formation of Subtropical Mode Water and Sub-Antarctic Mode Water in their respective zones. Between the north of the STF and the PZ, the growth rate of total dissolved inorganic carbon was calculated to be about 0.5–0.8 μmol kg^{-1} yr^{-1} via the buffer factor.

1. Introduction

The ocean plays an important role in determining the atmospheric CO_2 level, which has been currently increasing due to human activities (IPCC, 2001). Because of the large surface area and regional wind velocity, the Southern Ocean is considered to be an area showing a large CO_2 flux between the sea and the air (Sabine and Key, 1998). Furthermore, water formed in the Southern Ocean ventilates the intermediate and abyssal depths of much of the world's oceans (Rintoul and Bullister, 1999).

On the basis of measurements of the difference in the partial pressure (fugacity) of CO_2 between the sea and the overlying air (ΔpCO_2), CO_2 uptakes in the Southern Ocean south of 50°S were estimated to be in the range of 0.2 to 0.6 Gt-C yr^{-1} (Tans et al., 1990; Takahashi et al., 1997, 1999), while atmospheric inverse models, which use spatial distributions of atmospheric CO_2 for inferring surface CO_2 fluxes, gave lower atmospheric CO_2 uptakes of about 0.1 Gt-C yr^{-1} (Rayner et al., 1999). Takahashi et al. (2002) reported that the uptake of the Southern Ocean (south of 50°S) is greater than 20% of the total, although it occupies about 10% of the global ocean. However, most ΔpCO_2 measurements are made only in the Austral summer (see, for example, Metzl et al., 1999), which is insufficient to elucidate the annual CO_2 uptake in the Southern Ocean. A lower value of oceanic uptake close to that of the atmospheric inversion model and ocean inversion model (Gloor et al., 2003) has been estimated by adding the observed ΔpCO_2 data for the Austral winter (Metzl, after Fig. 1 of Roy et al., 2003). This does not reconcile the numerical model result of a small Southern Hemisphere CO_2 uptake with the observations because numerical model studies that examined the distributions of CO_2 sources and sinks have

*Corresponding author.
e-mail: hyoshika@ees.hokudai.ac.jp

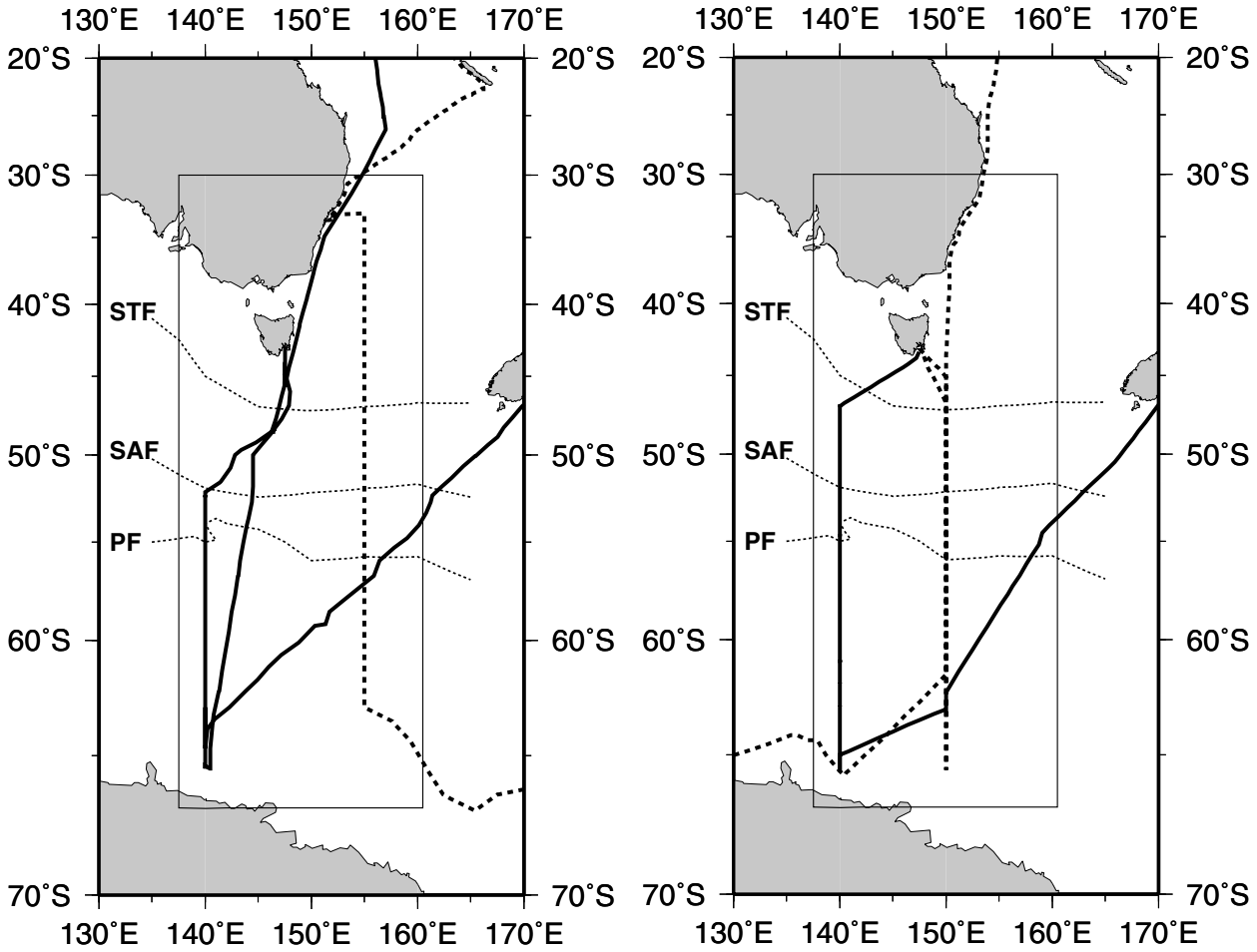

Fig 1. Cruise tracks of the R/V *Hakuho-maru* in the Southern Ocean. In the left panel, the dotted line shows the cruise track from December 1968 to February 1969, and the solid line that from December 1994 to January 1995. In the right panel, the dotted line shows the cruise track from December 1983 to January 1984, and the solid line that in January 2002. Temporal and spatial variations in pCO_2^{sw} were examined in the area surrounded by the thin solid line. The geographical position of the STF, SAF and PF was drawn on the basis of Sokolov and Rintoul (2002).

large uncertainties in estimating the regional CO_2 sources and sinks (Sabine and Key, 1998). As was pointed out by Roy et al. (2003), at present, potential errors in these estimates have not been quantified enough to claim consistency among various recent results.

By taking into account the annual cycle of the fugacity of CO_2 in surface seawater (fCO_2^{sw}), Metzl et al. (1999) suggested a CO_2 uptake of about 1 Gt-C yr^{-1} in the circumpolar Sub-Antarctic Zone (SAZ), which lies between the Subtropical Front (STF) and the Sub-Antarctic Front (SAF). Takahashi et al. (2002) estimated a CO_2 uptake of 1.51 Gt-C yr^{-1} between 14°S and 50°S, which was concentrated in the transition zone between the subtropical gyre and subpolar waters. Most atmospheric models gave a strong sink for atmospheric CO_2 at latitudes ∼30–50°S (Ciais et al., 1995; Enting et al., 1995; Rayner et al., 1999; Roy et al., 2003). On the basis of total dissolved inorganic carbon (DIC) data below 200 m measured in 1968 and 1996, McNeil et al., (2001) estimated an anthropogenic CO_2 uptake of 0.07–0.08 Gt-C yr^{-1} in the circumpolar SAZ, which is the area where deep penetration of anthropogenic CO_2 occurs (<1900 m). This corresponded to about 10% of the total annual CO_2 uptake in the circumpolar SAZ. They also reported that the anthropogenic CO_2 accumulated less across the Polar Frontal Zone (PFZ) toward the south and remained relatively constant from 53 to 58°S in the upper water column because of strong density gradients; furthermore, it accumulated significantly in the Antarctic Bottom Water, a dense water mass that sinks to abyssal depths along the Antarctic continental slope.

It is important to clarify the long-term trend of the carbonate system in surface seawater of the Southern Ocean, which has been thought to exhibit larger uptake rates, in order to understand the role in the global carbon budget. This will provide a constraint for the simulation of global carbon cycle models.

The thermodynamic effect, ocean transport (lateral flow, vertical mixing and upwelling of water), biological activity and CO_2 exchange between the sea and the overlying air are the

processes (Poisson et al., 1993; Lee et al., 1998) affecting the partial pressure of CO_2 of surface seawater via changes in the total DIC, total alkalinity, pH, temperature and salinity. One approach for evaluating the long-term trend due to the uptake of anthropogenic CO_2 is to compare the pCO_2^{sw} data taken at the same condition of the thermodynamics, ocean transport and biological activity. In order to attain these conditions, Feely et al. (1999) examined the long-term trend of pCO_2^{sw} for the core of upwelled water in the region of the temperature minimum near the equator, between 140 and 160°W, by using the pCO_2^{sw}–sea-surface temperature (SST) relationship.

The IPCC (2001) reported an increase of global SST in the Northern Hemisphere of 0.18 °C per decade and in the Southern Hemisphere of 0.10 °C per decade from 1976 to 2000. The rate of change in the observed pCO_2^{sw} over a few decades, therefore, can be caused by variations in all four processes mentioned above.

After correcting for SST changes and the annual uptake of atmospheric CO_2, Takahashi et al. (2003) reported the rates of change in pCO_2^{sw} in the central and western equatorial Pacific between the 1980s and 1990s. They determined that there were decreases in pCO_2^{sw} at a mean rate of -20 μatm per decade before the phase shift of the Pacific Decadal Oscillation (PDO) and increases at about 15 μatm per decade after that, which could be caused by variations in ocean transport and biological activity.

In this paper, the distributions and variations in (pCO_2^{sw}) in the Southern Ocean will be reported by using Austral summer (December–February) data measured in 1968–1969, 1983–1984, 1994–1995 and 2002; moreover, the long-term trend of pCO_2^{sw} and the uptake of anthropogenic CO_2 in the mixed layer will be discussed.

2. Experiment

As shown in Fig. 1, this study covered the region extending from 33°S to 66°S south of Australia. Data for pCO_2^{sw} and those for overlying air (pCO_2^{air}) were collected over the period from January to February 1969, December 1983 to January 1984, December 1994 to January 1995 and January 2002 along with auxiliary hydrographic data (Oceanographic Data of KH68-4 1970; Nakai et al., 1986; Kawaguchi, 1996; Terazaki et al., 2003). Analysis of DIC was made coulometrically using an automated CO_2 extraction unit and a coulometer for the cruises from December 1994 to January 1995 and January 2002 (Ishii et al., 1998; Ishii et al., 2002). The ship used was the R/V *Hakuho-maru*, which belongs to the Ocean Research Institute, University of Tokyo.

Underway measurements of pCO_2^{sw} and pCO_2^{air} for these cruises were carried out with systems reported earlier (Miyake et al., 1974; Inoue and Sugimura, 1988; Inoue, 2000; Körtzinger et al., 2000). For the four cruises, the heart of the underway measurements of pCO_2^{sw} and pCO_2^{air} was the same. They consisted of a non-dispersive infrared gas analyser, a shower-head-type equilibrator, diaphragm pumps and a unit for the removal of water vapour in sample air. Uncontaminated water from the inlet of sample seawater about 5 m below the surface was introduced into the equilibrator at approximately 10 l min^{-1}. CO_2 in the water is equilibrated with recirculated air in a shower-head-type equilibrator. Taking factors affecting pCO_2^{sw} measurements into account, we retrieved pCO_2^{sw} data measured in 1968–1969 and 1983–1984 to compare the results with those obtained most recently (Inoue et al., 1999). Four standard gases (typically 290, 340, 370, 420 ppm CO_2 in natural air, Nippon Sanso Co. Ltd) traceable to the World Meteorological Organization (WMO) mole fraction scale were used aboard the ship (Inoue et al., 1995; Inoue et al. 1999) during cruises in 1994–1995 and 2002. The partial pressure of CO_2 in the equilibrator (pCO_2^{eq}) was calculated from the CO_2 mole fraction in dry air equilibrated with seawater in the equilibrator (xCO_2^{eq}),

$$pCO_2^{eq} = xCO_2^{eq}(P_{bar} - W), \quad (1)$$

where P_{bar} is the barometric pressure at the air–sea boundary and W is the water vapour pressure equilibrated with seawater. In order to calculate pCO_2^{sw} from pCO_2^{eq}, we used the equation given by Gordon and Jones (1973) for the three cruises in 1968–1969, 1983–1984 and 1994–1995 and by Copin-Montégut (1988); Copin-Montégut (1989) for the cruise in 2002. The increase in temperature from the sea surface to the equilibrator was typically 0.7 °C in 1968–1969, 0.3 °C in 1983–1984, 0.5 °C in 1994–1995 and 0.4 °C in 2002. The two equations expressing the temperature dependence of pCO_2^{sw} might lead to a difference of 1 μatm, but this was within the estimated precision of measurements (better than 3.6 μatm; Inoue et al., 1999). Our results and discussion remain unchanged because they do not depend critically on the two different equations.

The barometric pressure varied spatially and temporally. For example, in the SAZ, P_{bar} ranged from 1007.1 to 1022.3 hPa with a median value of 1016.6 hPa in January 1969, 996.7 to 1026.3 hPa with 1000.1 hPa in December 1983–January 1984, 996.2 to 1029.2 hPa with 1017.3 hPa in December 1994–January 1995 and 1005.6 to 1011.5 hPa with 1009.2 hPa in January 2002. The observed barometric pressure is simply related to weather systems. In this work, we focused on variations in the carbonate system in the surface mixed layer. In order to avoid any effects of the weather system on the long-term variations in pCO_2^{air} and pCO_2^{sw}, we used an average P_{bar} in each zone for four cruises (see Sections 4.2 and 4.3).

The pCO_2^{sw} data for 1968–1969, 1983–1984 and 1994–1995 were sent to the WMO World Data Centre for Greenhouse Gases (WDCGG) (Tokyo, Japan), and those for 2002 will be sent in the near future.

3. Oceanographic setting

Three major fronts were observed south of 40°S (Rintoul et al., 1997; Rintoul and Bullister, 1999; Yaremchuk et al., 2001). The STF, marked as the boundary between warm, salty subtropical water and cool, fresh sub-Antarctic water, was located in the range of 44.5–46.5°S. The SAF, characterized by a steep

Table 1. Location of three major fronts south of Australia determined on the basis of hydrographic data (Oceanographic Data of KH68-4 1970; Nakai et al., 1986; Kawaguchi, 1996; Terazaki et al., 2003)

Year	Observation period	STF	SAF	PF	SSIZ[a]
1969	23 Jan–4 Feb	44.5°S, 155°E	51.5°S, 155°E	54°S, 155°E	62°S, 155°E
1983–1984	11 Dec–15 Jan	45.5°S, 150°E	49°S, 150°E	54.5°S, 150°E[b]	62°S, 150°E
1994–1995	15 Dec–27 Jan	45.5°S, 147°E	50°S, 142°E	51°S, 140°E	62°S, 140°E
2002	4 Jan–20 Jan	46.5°S, 141°E	49.5°S, 140°E	52.5°S, 140°E	62°S, 140°E

[a]Northern latitude of the SSIZ.
[b]In the PZ, the pCO_2^{sw} data with SSS higher than 34 should be removed.

horizontal temperature gradient, was found in the range of 49–51.5°S. This SAF marks the northern edge of the eastward-flowing Antarctic Circumpolar Current. The Polar Front (PF), which marks the steep temperature gradient of the surface seawater and the northern limit of water with a minimum temperature of less than 2 °C near 200 m depth, was found at 53–56.5°S. South of Australia, Rintoul and Bullister (1999) described two distinct deep-reaching fronts, one at 53°S and one between 57 and 59°S on the SR3 section of the World Ocean Circulation Experiment (WOCE). However, the southern branch was less clearly defined than the northern one. The PF used in this work corresponds to the northern branch of the PF.

Chaigneau and Morrow (2002) reported that the STF, SAF and PF determined by continuous measurements of SST and sea-surface salinity (SSS) between Tasmania and Antarctica were located further north than their subsurface counterparts. In this work, we will use the criteria given by Chaigneau and Morrow (2002) for available SST and SSS data, because we discuss the long-term trend of the carbonate system in surface seawater. Three major fronts observed for the four cruises are summarized in Table 1.

The zones between the fronts are commonly referred to as the SAZ between the STF and the SAF and the PFZ between the SAF and the PF. The Polar Zone (PZ) extends southward from the PF to the Antarctic Divergence, which may be called the Permanently Open Ocean Zone (POOZ, Tréguer and Jacques 1992). The Antarctic Divergence marks the transition from prevailing westerlies to coastal Antarctic easterlies as well as the location of upwelling of circumpolar deep water (Popp et al., 1999). However, the colder, less saline surface water close to the ice edge often overwhelmed the Antarctic Divergence (Ishii et al., 2002). The Seasonal Sea-Ice Zone (SSIZ) is the zone affected by the ice melt from receding sea ice (Popp et al., 1999). In this work, the northern boundary of the SSIZ was assumed to be 62°S on the basis of the distribution of surface salinity and satellite images (Enomoto and Ohmura, 1990).

4. Results and discussion

4.1. Distribution and seasonal variation in pCO_2^{sw}

Figure 2 illustrates the latitudinal distribution of pCO_2^{sw} in January–February 1969, January 1984, January 1995 and January 2002. North of the SAF, pCO_2^{sw} showed a coherent meridional pattern in the Austral summer. In the subtropics north of the STF, pCO_2^{sw} decreased towards the south as the SST decreased. The minimum pCO_2^{sw} occurred at 44.5°S in 1969 and

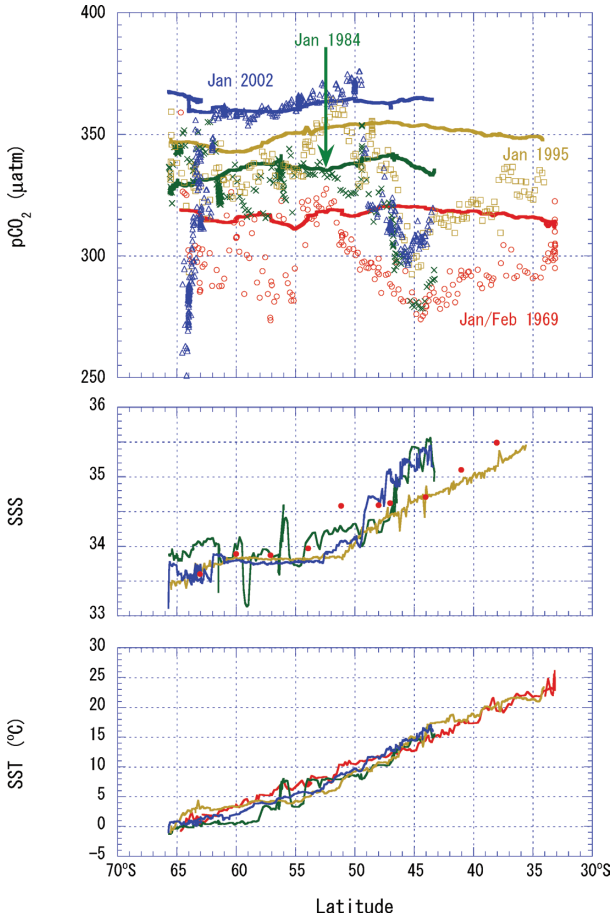

Fig 2. Latitudinal distributions of pCO_2^{air} and pCO_2^{sw}, SSS and SST observed in January–February 1969, January 1984, January 1995 and January 2002. In the upper panel, red open circles show the pCO_2^{sw} in January–February 1969, green crosses that in January 1984, brown open squares that in January 1995, and blue open triangles that in January 2002; the solid lines show the pCO_2^{air}. In the middle and lower panels the colour of the line is the same as that in the upper panel. In January 2002, the pCO_2^{sw} decreased steeply to the level of 150 μatm south of 65°S.

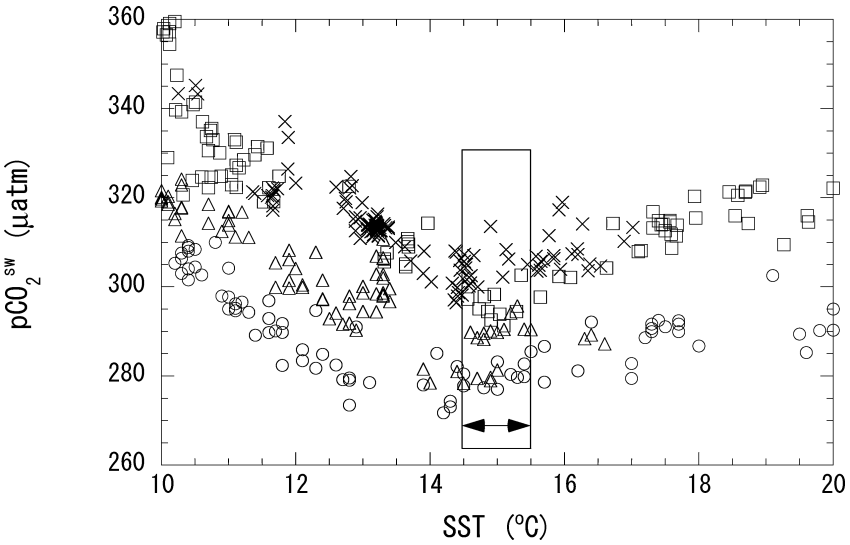

Fig 3. Temperature dependence of pCO_2^{sw} in the SST range between 10 and 20 °C for the subtropics and SAZ. Open circles show the pCO_2^{sw} in January 1969, open triangles that in January 1984, open squares that in January 1995, and cross symbols that in January 2002. The average pCO_2^{sw} surrounded by the thin solid line was used to calculate the pCO_2^{sw} minimum value north of the STF.

Table 2. The pCO_2^{sw}–SST relationships in the SAZ

Period	$pCO^2_{sw_*}$–SST relationship[a]		$1\sigma/\mu$atm	r
January 1969	$pCO_2^{sw} = (407.6 - 9.90) \times$ SST, $n = 43$,	$p < 0.001$	4.3	0.912
December 1983–January 1984	$pCO_2^{sw} = (404.7 - 8.30) \times$ SST, $n = 70$,	$p < 0.001$	6.1	0.858
December 1994–January 1995	$pCO_2^{sw} = (444.4 - 10.1) \times$ SST, $n = 121$,	$p < 0.001$	8.8	0.780
January 2002	$pCO_2^{sw} = (456.5 - 10.9) \times$ SST, $n = 82$,	$p < 0.001$	5.3	0.895

[a]In the SAZ, the average P_{bar} was 1012.5 hPa.

1984, 45°S in 1995 and 45.5°S in 2002. These were latitudes at the SST of ∼15 °C (Fig. 3), which was equal to the lower limit of temperature of the Subtropical Mode Waters (15–19 °C) in the southwestern Pacific Ocean (Roemmich and Cornuelle, 1992). Our results show that the minimum pCO_2^{sw} occurred slightly north of the STF or at the STF (Table 1). In this area, pCO_2^{sw} decreased due to the cooling of warm subtropical water and biological drawdown of CO_2 in the nutrient-rich subpolar waters (Takahashi et al., 2002).

In the area of the SAZ, pCO_2^{sw} increased toward the south as the SST decreased (Fig. 4). The pCO_2^{sw} data measured during repeated occasions in the Austral summer show that both temporal and spatial variations can be approximated well by a single pCO_2^{sw}–SST relationship for each cruise (Table 2). We will use the pCO_2^{sw}–SST relationship to elucidate the long-term increase of pCO_2^{sw} due to uptake of anthropogenic CO_2 (see Section 4.2).

The maximum pCO_2^{sw}, which was higher than pCO_2^{air}, occurred close to the SAF (Fig. 2), while Sabine and Key (1998) reported that the SAF was associated with a local minimum in fCO_2^{sw} along 126 and 88°W in December 1992 and January 1993. South of the maximum in pCO_2^{sw}, pCO_2^{sw} showed a distribution that differed from year to year (Fig. 2). In the PFZ, for example, the pCO_2^{sw} in January 1984 tended to increase towards the south, and, in January 2002, it decreased. In the PZ, the pCO_2^{sw} in January 1969 generally decreased to a lower level with large variability on small spatial scales. In January 1984 a local maximum of SSS occurred at 56°S, where corresponded to the subsurface PF (Chaigneau and Morrow, 2002). In this area the SSS increased along with the SST. Warm water with a high SSS and different carbonate system was probably transported southwards due to an eddy. Around the minimum SSS at 59°S the SST remained constant, and the pCO_2^{sw} decreased with the decrease in SSS. In January 2002, the pCO_2^{sw} in the PZ was remarkably constant and equal to pCO_2^{air}. In the SSIZ, the pCO_2^{sw} in January 2002 decreased significantly toward the south from 360 to 150 μatm along with decreases in macronutrients (Terazaki et al., 2003); this was associated with the CO_2 uptake due to the biological activity in summer (Poisson et al., 1994). Metzl et al. (1999) showed a pattern similar to that of January 2002, i.e. changes from 370 to 230 μatm along 30°E and from 370 to 270 μatm along 145°E in February–March 1993 (the fCO_2^{sw} values were taken from Fig. 2 of Metzl et al., 1999). In January 2002, temperature and salinity data indicated that waters showing steep changes in pCO_2^{sw} and macronutrients were associated with an eddy and had been transported from an area close to Antarctica (Aoki, personal communication).

Inoue and Sugimura (1988) reported that the pCO_2^{sw} in the PFZ, PZ and SSIZ remained almost constant for about 1 month,

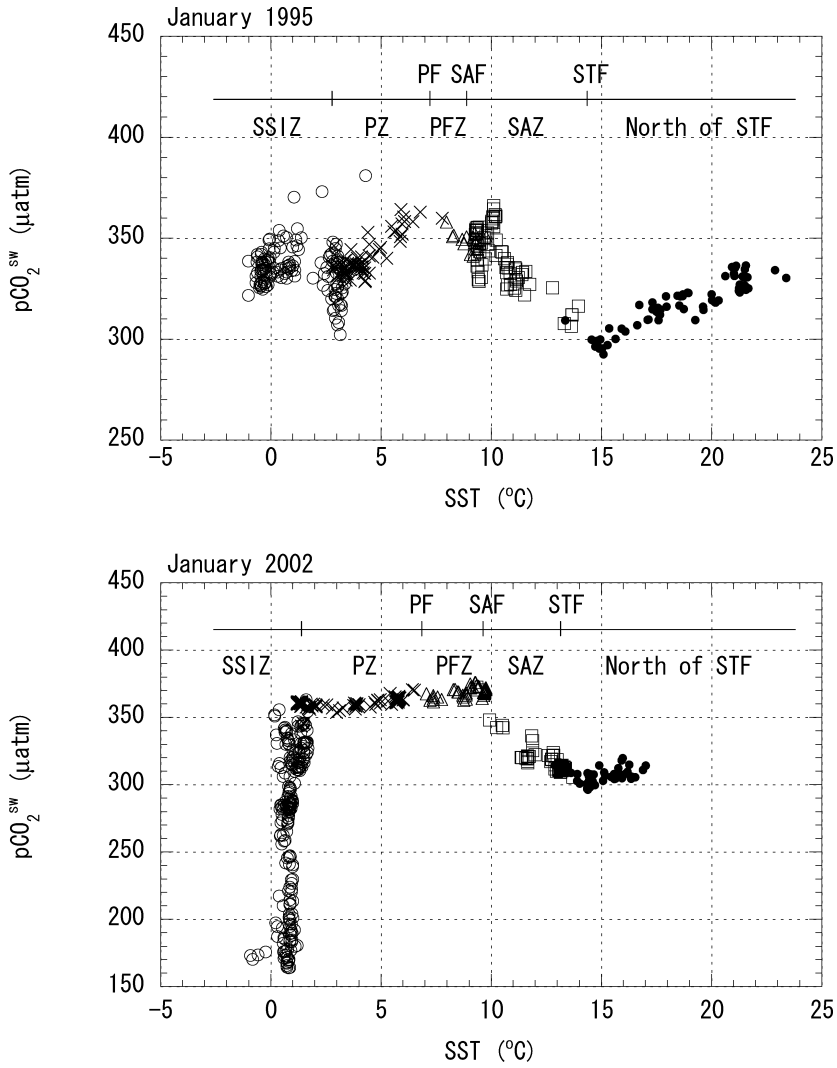

Fig 4. Temperature dependence of the pCO_2^{sw} in the area north of the STF to the SSIZ measured in January 1995 (upper panel) and January 2002 (lower panel). Open circles show the data measured in the SSIZ, crosses those in the PZ, open triangles those in the PFZ, open squares those in the SAZ, and solid circles those in the north of the STF.

starting from the middle of December 1983. In these zones, pCO_2^{sw} also remained fairly constant from December 1994 to January 1995 and in January 2002. The pCO_2^{sw} in the Austral summer varied independently from changes in the SST, both spatially and temporally (Fig. 4), mainly due to variations in the rise in SST and carbon uptake by biological activity (Ishii et al. 1998; Ishii et al. 2002).

4.2. *Long-term trend of the pCO_2^{sw} in the Southern Ocean*

In the Southern Ocean, major fronts shifted interannually and longitudinally (Table 1). This would lead to a large error if we tried to evaluate the long-term trend of pCO_2^{sw} at the given geographical position close to the major front. If the same water mass remained at that location for a few decades, we could calculate the long-term trend of pCO_2^{sw} at fixed latitudes. However, selecting the latitude covered with the same water mass considerably decreases the number of available data. For example, in the SAZ only a small number of data (around 48°S) were available in January 1969 and January 1984. Therefore, we determined the representative pCO_2^{sw} value in the water mass with uniform properties in each zone by using pCO_2^{sw} data as much as possible and evaluating the long-term trend in the Southern Ocean.

We summarize pCO_2^{air}, pCO_2^{sw} and thermodynamically temperature-normalized pCO_2^{sw} (N-pCO_2^{sw}) in each zone measured in January (Table 3). The increases of the pCO_2^{sw} minimum at the SST of 15 °C north of the STF were always smaller than those of pCO_2^{air}. South of SAZ, the variations in pCO_2^{sw} differ largely not only from those of pCO_2^{air} but also those of adjacent zones (Table 3). The N-pCO_2^{sw} at an average SST for each zone tended to vary more than pCO_2^{sw}. The larger variability of the N-pCO_2^{sw} was due to the removal of the thermodynamic temperature effect, which compensates for the effect of the ocean transport and biological activity on pCO_2^{sw}. The pCO_2^{sw} and N-pCO_2^{sw} data show large interannual/decadal variations superimposed on the long-term increase. However, the present data were not sufficient to examine interannual/decadal variations in the carbonate

Table 3. The pCO_2^{air}, pCO_2^{sw}, N-pCO_2^{sw} and SST in the area of the pCO_2^{sw} minimum north of the STF, SAZ, PFZ, PZ and SSIZ in January observed for the period from 1969 to 2002. Differences in pCO_2^{air}, pCO_2^{sw} and N-pCO_2^{sw} between two cruises are given by Δ^{air}, Δ^{sw} and N-Δ^{sw} respectively. The N-pCO_2^{sw} was calculated at the average SST of 11.4 °C for four cruises in the SAZ, the average SST of 8.7 °C in the PFZ, the average SST of 3.8 °C in the PZ, and the average SST of 0.9 °C in the SSIZ

Period	pCO_2^{air} (μatm)[a]	Δ^{air} (μatm)	pCO_2^{sw} (μatm)[a]	Δ^{sw} (μatm)	N-pCO_2^{sw} (μatm)	N-Δ^{sw} (μatm)	SST (°C)
pCO_2^{sw} minimum at 15 °C north of the STF[b]							
1969[c]	317.2 ± 0.1, $n = 10$		280.4 ± 2.7, $n = 10$				14.5–15.5
1984	336.9 ± 0.7, $n = 15$	19.7 ± 0.7	287.2 ± 5.7, $n = 16$	6.8 ± 6.3			14.5–15.5
1995	351.9 ± 0.3, $n = 11$	15.0 ± 0.8	295.8 ± 3.3, $n = 10$	8.6 ± 6.6			14.5–15.5
2002	364.1 ± 0.2, $n = 21$	12.2 ± 0.3	304.5 ± 3.5, $n = 16$	8.7 ± 6.6			14.5–15.5
SAZ							
1969[c]	317.7 ± 0.3, $n = 44$		294.1 ± 10.3, $n = 43$		292.9		11.5 ± 1.0, $n = 44$
1984	337.8 ± 0.5, $n = 21$	20.1 ± 0.6	315.5 ± 11.0, $n = 21$	21.4 ± 15.1	316.8	23.9	11.0 ± 1.5, $n = 21$
1995	352.7 ± 0.5, $n = 40$	14.9 ± 0.7	337.9 ± 13.3, $n = 39$	22.4 ± 17.3	357.0	40.2	10.3 ± 1.4, $n = 39$
2002	363.8 ± 0.4, $n = 36$	11.1 ± 0.6	318.9 ± 11.7, $n = 82$	-19.0 ± 17.7	303.1	-53.9	12.6 ± 1.0, $n = 82$
			pCO_2^{sw}–SST				
1969[c]			294.7 ± 4.3, $n = 44$				11.5 ± 1.0, $n = 44$
1984			310.1 ± 6.1, $n = 76$	15.4 ± 7.5			11.3 ± 1.3, $n = 76$
1995			329.3 ± 8.8, $n = 121$	19.2 ± 10.7			10.1 ± 1.1, $n = 121$
2002			332.2 ± 5.3, $n = 122$	2.9 ± 10.2			12.6 ± 0.9, $n = 122$
PFZ							
1969[c]	316.8 ± 0.1, $n = 17$		318.9 ± 4.1, $n = 16$		328.5		8.0 ± 0.6, $n = 16$
1984	336.5 ± 0.5, $n = 33$	19.7 ± 0.5	326.9 ± 9.3, $n = 19$	8.0 ± 10.2	326.9	-1.6	8.7 ± 0.9, $n = 33$
1995	351.1 ± 0.3, $n = 16$	14.6 ± 0.6	348.1 ± 4.6, $n = 15$	21.2 ± 10.4	343.7	16.8	9.0 ± 0.5, $n = 15$
2002	363.0 ± 0.3, $n = 32$	11.9 ± 0.4	368.0 ± 2.9, $n = 62$	19.9 ± 5.4	360.3	16.6	9.2 ± 0.8, $n = 62$
PZ							
1969[c]	314.4 ± 0.3, $n = 47$		298.5 ± 14.7, $n = 44$		284.9		4.9 ± 1.7, $n = 47$
1984	335.0 ± 0.6, $n = 36$	20.6 ± 0.7	331.9 ± 6.7, $n = 62$	33.4 ± 0.7	343.3	58.4	3.0 ± 2.7, $n = 62$
1995	348.8 ± 0.7, $n = 151$	13.8 ± 0.9	340.6 ± 6.9, $n = 152$	8.7 ± 9.6	334.9	-8.4	4.2 ± 1.1, $n = 152$
2002	361.1 ± 0.4, $n = 126$	12.3 ± 0.8	361.6 ± 3.2, $n = 255$	21.0 ± 7.6	370.9	36.0	3.2 ± 2.0, $n = 255$
SSIZ[d]							
1969[c]	314.6 ± 0.1, $n = 21$		298.5 (282.7, 354.4), $n = 21$		296.0		1.0 ± 0.8, $n = 21$
1984	334.7 ± 0.6, $n = 29$	20.1 ± 0.6	340.0 (326.2, 345.9), $n = 36$	41.5	347.3	51.3	0.4 ± 0.6, $n = 36$
1995	348.9 ± 0.4, $n = 262$	14.2 ± 0.7	337.7 (333.1, 343.8), $n = 270$	-2.3	334.9	-12.4	1.1 ± 1.5, $n = 270$
2002	360.6 ± 0.3, $n = 232$	11.7 ± 0.5	282.2 (218.2, 318.5), $n = 480$	-55.5	282.2	-52.7	0.9 ± 0.4, $n = 722$
2002[e]	360.7 ± 0.2, $n = 81$	11.8 ± 0.4	326.1 (316.6, 337.1), $n = 167$	-11.6	322.0	-12.9	1.2 ± 0.3, $n = 253$

[a]The average barometric pressure used was 1014.5 hPa in the area close to the STF, 1006.9 hPa in the PFZ, 997.3 hPa in the PZ and 996.1 hPa in the SSIZ.

[b]Average pCO_2^{sw} for SSTs between 14.5 and 15.5 °C. The selection of the temperature range does not considerably affect the results. If we select the SST range between 14 and 16 °C, the average pCO_2^{sw} is 281.4 ± 4.1 μatm ($n = 17$) for January 1969, 286.4 ± 5.9 μatm ($n = 18$) for January 1984, 298.5 ± 3.9 μ atm ($n = 12$) for January 1995 and 304.9 ± 5.2 μatm ($n = 41$) for January 2002.

[c]In 1969, we used the atmospheric CO_2 data at baseline stations (Inoue et al. 1999).

[d]We examined the frequency distribution of the pCO_2^{sw} in the SSIZ. In January 2002, the frequency distribution of the pCO_2^{sw} showed a different pattern from that of the normal distribution. In the SSIZ, therefore, the median of the pCO_2^{sw} is given along with the 25th and 75th percentiles.

[e]62°S − 63.5°S.

system in the surface mixed layer of the Southern Ocean. In this work, therefore, we decided to work out the average feature of the long-term pCO_2^{sw} increase. By assuming a linear long-term trend of pCO_2^{sw}, we calculated the growth rate of pCO_2^{sw} in each zone (Table 4).

Here, we adiabatically divide the variations in pCO_2^{sw} into those of the processes affecting pCO_2^{sw}: the uptake of anthropogenic CO_2, variations in thermodynamics, ocean transport and biological activity. In Table 4, we list the rate of change in pCO_2^{sw} due to the long-term increase of SST (0.10 °C per decade; IPCC 2001) on the basis of the thermodynamic temperature effect (4.23% °C^{-1} Takahashi et al., 2003).

The growth rate of the observed pCO_2^{sw} tended to increase towards the south from the north of the STF, where the pCO_2^{sw}

Table 4. Rates of change of pCO_2^{air} and pCO_2^{sw} (μatm yr^{-1}) in the zone between major fronts of the Southern Ocean

Rate of change[a]	$\delta pCO_2^{air}/\delta t$	$\delta pCO_2^{sw}/\delta t$[b]	δpCO_2^{sw}(A_CO_2)$/\delta t$	δpCO_2^{sw}(Thermo)$/\delta t$	δpCO_2^{sw}(O_bio)$/\delta t$
pCO_2^{sw} minimum	1.4 ± 0.1	0.7 ± 0.1	0.7 ± 0.1		
SAZ	1.4 ± 0.1	1.0 ± 0.5 (0.8 ± 1.2)	1.2 ± 0.1[c]	0.1 ± 0.1	-0.3 ± 0.5
PFZ	1.4 ± 0.1	1.5 ± 0.4 (0.9 ± 0.4)		0.1 ± 0.1	
PZ	1.4 ± 0.1	1.8 ± 0.2 (2.3 ± 0.7)		0.1 ± 0.1	
SSIZ[d]	1.4 ± 0.1	0.8 ± 0.8 (0.7 ± 0.9)		0.1 ± 0.1	

[a]The rates of change in pCO_2^{air} and pCO_2^{sw} are expressed as $\delta pCO_2^{sw}/\delta t$. In parentheses, A_$CO_2$ means the annual uptake of anthropogenic CO_2, Thermo, the thermodynamic temperature effect due to the SST increase in the Southern Hemisphere (0.1 ± 0.05 °C per decade) and O_bio, the ocean transport and biological activity.

[b]The rate of change in N-pCO_2^{sw} is given in parentheses along with a standard deviation. The N-pCO_2^{sw} was normalized to the average SST in each zone for four cruises (Table 3).

[c]We used the pCO_2^{sw}–SST relationship to evaluate pCO_2^{sw} at the same SST for four cruises (11.4 °C).

[d]In January 2002, the pCO_2^{sw} data between 62 and 63.5°S were used. If all pCO_2^{sw} data were used, the long-term trend of pCO_2^{sw} would be calculated as -0.1 ± 1.4 μatm yr^{-1}. If we omitted the pCO_2^{sw} data for January 2002, it would be 1.6 ± 0.8 μatm yr^{-1}.

minimum occurs, to the PZ (Fig. 5). The pCO_2^{sw} minimum increased at a rate of 0.7 μatm yr^{-1}, which was half of the raet fo increase of pCO_2^{air} (1.4 μatm yr^{-1}) over the same period. In the SAZ, the growth rate of the observed pCO_2^{sw} was 1.0 μatm yr^{-1}, which could be affected by the annual uptake of anthropogenic CO_2 as well as by the thermodynamics, ocean transport and biological activity. We calculated the pCO_2^{sw} value at the same SST on the basis of the pCO_2^{sw}–SST relationship for each cruise (Table 2). Because, either directly or indirectly, the thermodynamics, ocean transport and biological activity are correlated with the SST (Lee et al. 1998), the pCO_2^{sw} at the same SST might allow us to evaluate the pCO_2^{sw} increase under the same conditions: the pCO_2^{sw} increase can be caused by the annual uptake of anthropogenic CO_2. If pCO_2^{sw} were calculated at exactly the same conditions, the growth rate of pCO_2^{sw} due to the annual uptake of anthropogenic CO_2 should remain constant against a given SST. Within a standard deviation (±1.0 °C) of the mean SST for four cruises (11.4 °C), the growth rate of pCO_2^{sw} remained constant (1.2 μatm yr^{-1}). The growth rate of pCO_2^{sw} due to the thermodynamic temperature effect is calculated to be 0.1 μatm yr^{-1}. Therefore, the effect of the ocean transport and biological activity due to the SST increase is estimated to be -0.3 ± 0.5 μatm yr^{-1}. The rate of change in N-pCO_2^{sw} (0.8 μatm yr^{-1}) could be caused by the annual uptake of anthropogenic CO_2, ocean transport and biological activity, as mentioned by Takahashi et al. 2003. In the SAZ, the growth rate of pCO_2^{sw} at the same SST was slightly lower than that of pCO_2^{air}. The relatively lower value of the long-term trend is probably caused by the formation of Sub-Antarctic Mode Water in this zone (McNeil et al., 2001). Because of increases in ΔpCO_2, the area at SST of ∼15 °C north of the STF and SAZ can be oceanic sinks for atmospheric CO_2, where the uptake of anthropogenic CO_2 has been increasing (Le Quéré et al., 2003).

In the PFZ, the growth rate of pCO_2^{sw} was nearly equal to that of pCO_2^{air}, and, in the PZ, the rate was slightly larger than that of pCO_2^{air} and pCO_2^{sw} reached the same level as that of the pCO_2^{air} in January 2002. In the SSIZ, the distribution of the pCO_2^{sw} in January 2002 differed remarkably from those obtained on the other three cruises due to the CO_2 uptake due to biological activity, which was supported by the steep changes in macronutrients. For example, the concentration of nitrate in surface seawater decreased from 25 μmol kg^{-1} at 62°S to 14 μmol kg^{-1} at 65°S. The limited data and distribution did not allow us to evaluate the long-term trend clearly. If we selected the pCO_2^{sw} data between 62 and 63.5°S, where the macronutrients in surface seawater were comparable (23 μmol kg^{-1} at 63.5°S) to those of the three cruises in the SSIZ, we would obtain a growth rate of 0.8 ± 0.8 μatm yr^{-1}.

4.3. Annual uptake of anthropogenic CO_2

Takahashi et al. (2003) implicitly assumed the increase of pCO_2^{sw} caused by the uptake of anthropogenic CO_2 (1.5 μatm yr^{-1}) in the central and western equatorial Pacific and determined the pCO_2^{sw} variations before and after the PDO shift. Our objective in this work is to elucidate the increase of pCO_2^{sw} caused by the uptake of anthropogenic CO_2. In the Southern Hemisphere, the absolute value of the variation in SST is smaller than that in the central and western equatorial Pacific, reported to be in the range between −0.03 and 0.1 °C yr^{-1} (Takahashi et al., 2003). After 1991, a slower rate of SST increase was reported in the area where this study was conducted (IPCC, 2001). This suggests relatively small long-term variations in pCO_2^{sw} due to variations in ocean transport and biological activity. Hereafter, we assume that the effect of ocean transport and biological activity on the long-term increase in pCO_2^{sw} offsets that of thermodynamics.

On the basis of DIC, pCO_2^{sw}, SST and SSS data measured in January 2002, we evaluated the rate of the DIC increase (Table 5) via the buffer factor (DOE 1994). The buffer factor in

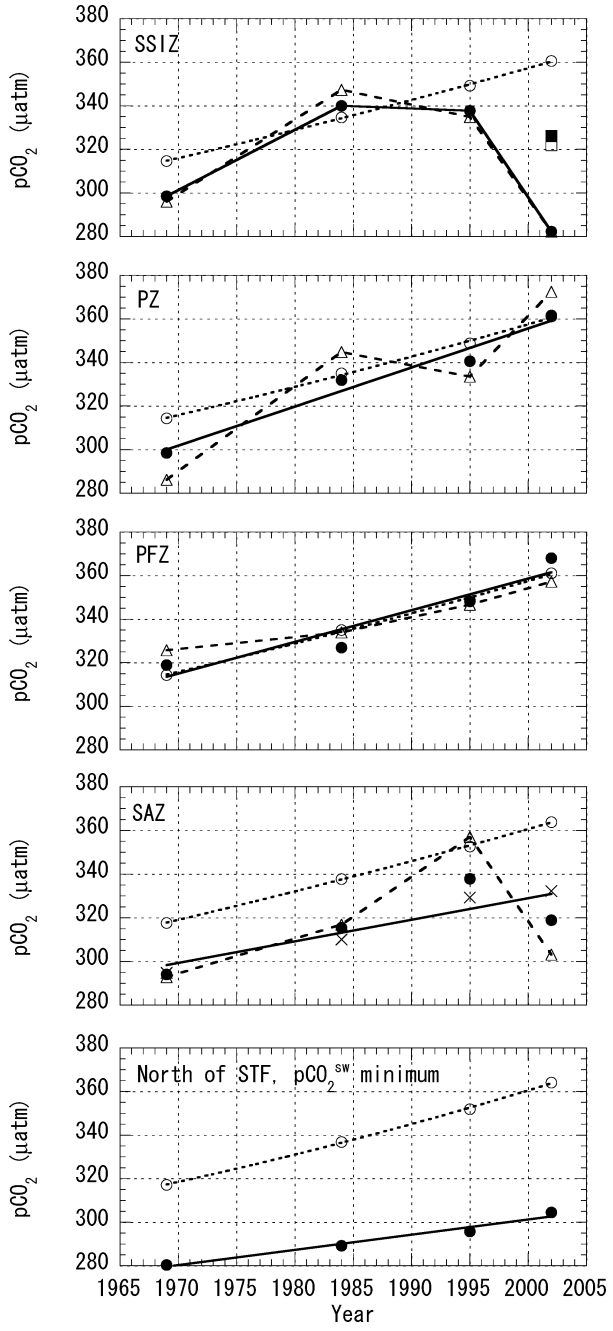

Fig 5. Variations in the pCO_2^{air} and pCO_2^{sw} in the area from the pCO_2^{sw} minimum at the SST of 15 °C north of the STF to the SSIZ during the period from 1969 to 2002. Open circles show the pCO_2^{air}, solid circles the pCO_2^{sw}, and open triangles the N-pCO_2^{sw}. The dotted line shows the long-term trend of pCO_2^{air} expressed as the second-degree polynomial function, the solid line the linear long-term trend of the pCO_2^{sw}, and the dashed line changes in N-pCO_2^{sw} between two cruises. In the SAZ, the crosses show the pCO_2^{sw} calculated by using the pCO_2^{sw}–SST relationship; in the SSIZ, the solid square shows the pCO_2^{sw} between 62 and 63.5°S and the open square the N-pCO_2^{sw} between 62 and 63.5°S.

this work was calculated to be in the range from 9.9 close to the STF and 14.4 in the SSIZ. The growth rate of the DIC was 0.5–0.8 μmol kg^{-1} yr^{-1} between the area close to the STF and the PZ. If we assume that the growth rate of DIC in surface seawater is equal to that of the mixed layer, we can evaluate the annual uptake of anthropogenic CO_2 in the mixed layer. In this work, the mixed layer depth (MLD) was taken from McNeil et al. (2001). Extrapolating our estimate of the DIC increase to the circumpolar zones, the annual uptake of anthropogenic CO_2 in the mixed layer can be estimated to be 0.17 Gt-C yr^{-1} in the SAZ and 0.03 Gt-C yr^{-1} in the PFZ and PZ (Table 6). McNeil et al. (2001) estimated that the circumpolar anthropogenic CO_2 uptake for the area between 45 and 50°S (SAZ) is 0.07–0.08 Gt-C yr^{-1}. Because of the vertical transport of CO_2 to the middle/deep water, our estimate is the lower limit of the CO_2 uptake in the Southern Ocean south of the STF. The estimation given in this work is the first step toward the precise estimation of the anthropogenic CO_2 uptake in the mixed layer of the Southern Ocean. It is necessary to observe the carbonate system in the wide area of the Southern Ocean systematically and repeatedly in order to better understand the oceanic uptake of anthropogenic CO_2 as well as the natural variability of the carbon cycle on a time scale of months to a few decades.

5. Summary

On the basis of Austral summer data of pCO_2^{air} and pCO_2^{sw} measured in 1968–1969, 1983–1984, 1994–1995 and 2002, we have reported the distributions and long-term variations in $pCO^{sw}{}_2$ in the Southern Ocean by dividing it into five zones between major fronts. Prior to this work, Inoue and Sugimura (1988) reported that the pCO_2^{sw} in high latitudes increased much more than in lower latitudes by comparing pCO_2^{sw} data between 1968–1969 and 1983–1984, and Inoue et al. (1999) suggested large interannual/decadal variations in the pCO_2^{sw} south of the STF.

By adding the pCO_2^{air} and pCO_2^{sw} data in January 2002 to these three data sets, we could discuss the spatial distribution of the long-term trend of pCO_2^{sw}. The growth rate of the pCO_2^{sw} minimum at the SST of 15 °C north of the STF was calculated to be a half (0.7 ± 0.1 μatm yr^{-1}) that of pCO_2^{air} (1.4 ± 0.1 μatm yr^{-1}). The observed growth rate of pCO_2^{sw} tended to increase from the SAZ (1.0 ± 0.5 μatm yr^{-1}) to the PZ (1.8 ± 0.2 μatm yr^{-1}). From 1976 to 2000, a time which was nearly equal to the period of our work, the SST in the Southern Hemisphere increased at a rate of 0.10 °C per decade, though the increase in high latitudes could be low (IPCC 2001). This suggests that the rate of pCO_2^{sw} increase is caused by the uptake of anthropogenic CO_2 as well as variations in the thermodynamics, ocean transport and biological activity.

The relatively low growth rates of pCO_2^{sw} minimum north of the STF and that in the SAZ are probably associated with the formation of Subtropical Mode Water and Sub-Antarctic Mode

Table 5. Growth rate of DIC in the surface seawater of the Southern Ocean, which was calculated on the basis of the growth rate of the pCO_2^{sw}, DIC, SST and SSS data measured in January 1995 and 2002

Zone	SST (°C)	SSS	pCO_2^{sw} (μatm)	$\delta pCO_2^{sw}(A\_CO_2)/\delta t$ (μatm yr^{-1})	N-DIC[a] (μ mol kg^{-1})	Buffer factor	$\delta DIC(A\_CO_2)/\delta t$ (μmol kg^{-1} yr^{-1})
pCO_2^{sw} minimum[b]	15.0	34.92	295.8	0.7 ± 0.1	1975.1	9.9	0.47 ± 0.14
SAZ	12.6	34.86	318.9	1.2 ± 0.1	2013.4	10.7	0.71 ± 0.09
PFZ	9.2	34.07	368.0	1.7 ± 0.4	2094.9	12.3	0.69 ± 0.27
PZ	3.2	33.82	361.6	2.0 ± 0.2	2138.2	14.1	0.75 ± 0.11
SSIZ	1.2	33.65	326.1	(1.0 ± 0.8)	2149.6	14.4	(0.37 ± 1.00)

[a]Normalized to an SSS of 34.
[b]Data in January 1995.

Table 6. Anthropogenic CO_2 uptake in the mixed layer of the Southern Ocean

Zone	MLD[a] (m)	Area (10^6 km^2)	$\delta DIC(A\_CO_2)/\delta t$ (μmol kg^{-1} yr^{-1})	CO_2 uptake (Gt-C yr^{-1})
pCO_2^{sw} minimum	150		0.47 ± 0.14	
45–50°S	500	13.4	0.71 ± 0.09	0.058 ± 0.007
SAZ	500	39[b]	0.71 ± 0.09	0.17 ± 0.02
PFZ	500	3[c]	0.69 ± 0.27	0.013 ± 0.005
PZ	150	14[c]	0.75 ± 0.11	0.019 ± 0.003
SSIZ	(50)	16[c]	(0.37 ± 1.00)	(0.004 ± 0.011)

[a]Mixed layer depth, McNeil et al. (2001).
[b]Hoshiai (1982).
[c]Tréguer and Jacques (1992).

Water in their respective zones. The effect of the increasing atmospheric CO_2 on pCO_2^{sw} is relatively low due to waters with a deep mixed layer as compared with those of the subtropics, where pCO_2^{sw} has been increasing at a rate parallel with or larger than that of pCO_2^{air} (Inoue et al., 1995; Inoue et al., 1999; Bates, 2001; Dore et al. 2003). In the SSIZ, because of the large effect of biological activity in January 2002, we could not detect the long-term trend of pCO_2^{sw}. At high latitudes, continuous measurements of the concentrations of macronutrients, as well as of pCO_2^{sw}, must be conducted. Such measurements will allow us to estimate the contribution of biological activity on the carbonate system.

In the Southern Ocean, the long-term variations in pCO_2^{sw} are considered to be mostly caused by the uptake of anthropogenic CO_2. By using the buffer factor, we could estimate the growth rate of surface DIC in the range of 0.5–0.8 μmol kg^{-1} yr^{-1} between the area close to the STF and the PZ (Table 5). On the basis of the growth rate of the DIC, the annual uptake of anthropogenic CO_2 in the mixed layer, estimated as a first step, is 0.17 Gt-C yr^{-1} in the SAZ and 0.03 Gt-C yr^{-1} in the PFZ and the PZ. This leads to the lower limit of the annual uptake of anthropogenic CO_2 in the Southern Ocean because CO_2 transferred from the surface mixed layer to the deeper layer was not taken into account. In order to evaluate the total annual uptake of CO_2 in the Southern Ocean more precisely, it is necessary to examine the temporal and spatial (vertical) distribution of the carbonate system in the wide area of the Southern Ocean repeatedly and systematically over a few decades at least.

6. Acknowledgments

We wish to thank Professor Terazaki of the Ocean Research Institute/University of Tokyo who served as a chief scientist KH-01-3 cruise and officers and crew of the R/V *Hakuho-maru* for their help on board. Comments by two anonymous reviewers were highly appreciated. This work is partly supported by the grant from the "Global Carbon Cycle and Related Mapping based on Satellite Imagery Program (GCMAPS)" of the Ministry of Education, Culture, Sports, Science and Technology, Japan.

References

Bates, N. R. 2001. Interannual variability of oceanic CO_2 and biogeochemical properties in the Western North Atlantic subtropical gyre. *Deep-Sea Res. II* **48**(8–9), 1507–1528.

Chaigneau, A. and Morrow, R. 2002. Surface temperature and salinity variations between Tasmania and Antarctica, 1993–1999. *J. Geophys. Res.* **107**(C12), 8020, doi:10.1029/2001JC000808.

Ciais, P., Tans, P. P., Trolier, M., White, J. W. C. and Francey, R. J. 1995. A large Northern Hemisphere terrestrial CO_2 sink indicated by the $^{13}C/^{12}C$ ratio of atmospheric CO_2. *Science* **269**, 1098–1102.

Copin-Montégut, C. 1988. A new formula for the effect of temperature on the partial pressure of CO_2 in seawater. *Mar. Chem.* **25**, 29–37.

Copin-Montégut, C. 1989. A new formula for the effect of temperature on the partial pressure of CO_2 in seawater. Corrigendum. *Mar. Chem.* **27**, 143–144.

DOE 1994. *Handbook of Methods for the Analysis of the Various Parameters of the Carbon Dioxide System in Sea Water; Version 2* (edsA. G. Dickson and C. Goyet) ORNL/CDIAC-74. Oak Ridge National Laboratory, Oak Ridge, TN.

Dore, J. E., Lukas, R., Sadler, D. W. and Karl, D. M. 2003. Climate-driven changes to the atmospheric CO_2 sink in the subtropical North Pacific Ocean. *Nature*, **424**, 754–757.

Enting, I. G., Trudinger C. M. and Francey, R. J. 1995. A synthesis inversion of the concentration and $\delta^{13}C$ of atmospheric CO_2. *Tellus* **47B**, 35–52.

Enomoto, H. and Ohmura, A. 1990. The influence of atmospheric half-yearly cycle on the sea ice extent in the Antarctic. *J. Geophys. Res.* **95**, 9497–9511.

Feely, R. A., Wanninkhof, R., Takahashi, T. and Tans, P. P. 1999. Influence of El Niño on the equatorial Pacific contribution to atmospheric CO_2 accumulation. *Nature* **398**, 597–601.

Gloor, M., Gruber, N., Sarmiento, J., Sabine, C. L., Feely, R. A. et al. 2003. A first estimate of present and preindustrial air–sea CO_2 flux patterns based on ocean interior carbon measurements and models. *Geophys. Res. Lett.* **30**(1), 1010, doi:10.1029/2002GL015594.

Gordon, L. I. and Jones, L. B. 1973. The effect of temperature on carbon dioxide partial pressure in sea water. *Mar. Chem.* **1**, 317–322.

Hoshiai, T. 1982. Ecosystem in the Southern Ocean. In: *Science in Antarctica. 7. Biology* (ed. T. Matsuda). Kokon Shoin, Tokyo, 4–11.

Inoue, H. Y. 2000. CO_2 exchange between the atmosphere and the ocean. Carbon dioxide studies of the Meteorological Research Institute since 1968. In: *Dynamics and Characterization of Marine Organic Matter* (eds. N. Handa, E. Tanoue and T. Hama). Terrapub/Kluwer, Tokyo, 509–531.

Inoue, H. Y., Ishii, M., Matsueda, H., Saito, S., Midorikawa, T. et al. 1999. Partial pressure of CO_2 in surface waters of the Pacific during 1968 to 1970: re-evaluation and comparison of data. *Tellus* **51B**, 830–848.

Inoue, H. Y., Matsueda, H., Ishii, M., Fushimi, K., Hirota, M. et al. 1995. Long-term trend of the partial pressure of carbon dioxide (pCO_2) in surface waters of the western North Pacific, 1984–1993. *Tellus* **47B**, 391–413.

Inoue, H. and Sugimura, Y. 1988. Distribution and variation of carbon dioxide in the western North Pacific, eastern Indian, and Southern Ocean, south of Australia. *Tellus* **40B**, 308–320.

IPCC. 2001. *Climate Change 2001: The Scientific Basis* (edsJ. T. Houghton, Y. Ding, D. J. Griggs, M. Noguer, P. J. van der Linden et al.). Cambridge University Press, Cambridge.

Ishii, M., Inoue, H. Y. and Matsueda, H. 2002. Net community production in the marginal ice zone and its importance for the variability of the oceanic pCO_2 in the Southern Ocean south of Australia. *Deep-Sea Res. II* **49**, 1691–1706.

Ishii, M., Inoue, H. Y., Matsueda, H. and Tanoue, E. 1998. Close coupling between seasonal biological production and dynamics of dissolved inorganic carbon in the Indian Ocean sector and the western Pacific Ocean sector of the Antarctic Ocean. *Deep-Sea Res. I* **45**, 1187–1209.

Kawaguchi, K. 1996. *Preliminary Report of the R/V Hakuho Maru Cruise KH-94-4. Southern Ocean Expedition*. Ocean Research Institute, University of Tokyo.

Körtzinger, A., Mintrop, L., Wallance, D. W. R., Johnson, K. M., Neill, C. et al. 2000. The international at-sea intercomparison of fCO_2 systems during the R/V Meteor Cruise 36/1 in the North Atlantic Ocean. *Mar. Chem.* **72**, 171–192.

Lee, K., Wanninkhof, R., Takahashi, T., Doney, S. C. and Feely, R. A. 1998. Low interannual variability in recent oceanic uptake of atmospheric carbon dioxide. *Nature* **396**, 155–159.

Le Quéré, C., Aumont, O., Bopp, L., Bousquet, P., Ciais, P. et al. 2003. Two decades of ocean CO_2 sink and variability. *Tellus* **55B**, 649–656.

McNeil, B. I., Tilbrook, B. and Matear, R. J. 2001. Accumulation and uptake of anthropogenic CO_2 in the Southern Ocean, south of Australia between 1968 and 1996. *J. Geophys. Res.* **106**(C12), 31 431–31 445.

Metzl, N., Tilbrook, B. and Poisson, A. 1999. The annual fCO_2 cycle in the Subantarctic Ocean. *Tellus* **51B**, 849–861.

Miyake, Y., Sugimura, Y. and Saruhashi, K. 1974. The carbon dioxide content in the surface water in the Pacific Ocean. *Rec. Oceanogr. Wks. Japan* **12**, 45–52.

Nakai, T., Hasumoto, H. and Nemoto, T. 1986. Oceanographic conditions of the Australian sector of the Southern Ocean in the summer of 1983–84. *Mem. Natl. Inst. Polar Res., Spec. Issue* **40**, 467–478.

Oceanographic Data of KH68-4. 1970. *Oceanographic Data of KH68-4 (Southern Cross Cruise) of the Hakuho Maru*. Ocean Research Institute, University of Tokyo.

Poisson, A., Metzl, N., Brunet, C., Schauer, B., Bres, B. et al. 1993. Variability of sources and sinks of CO_2 in the western Indian and Southern Oceans during the year 1991. *J. Geophys. Res.* **98**, 22 759–22 778.

Poisson, A., Metzl, N., Danet, X., Louanchi, F., Brunet, C. et al. 1994. Air–sea CO_2 fluxes in the Southern Ocean between 25° and 85°E. In: *The Polar Oceans and their Role in Shaping the Global Environment*, AGU Geophysical Monograph 85 (eds O. M. Johannessen, R. D. Muenchi and J. E. Overland). American Geophysical Union, Washington, DC, 273–284.

Popp, B. N., Trull, T., Kenig, F., Wakeham, S. G., Rust, T. M. et al. 1999. Controls on the carbon isotopic composition of Southern Ocean phytoplankton. *Global Biogeochem. Cycles* **13**, 827–843.

Rayner, P. J., Enting, I. G., Francey, R. J. and Langenfelds, R. L. 1999. Reconstructing the recent carbon cycle from atmospheric CO_2, $\delta^{13}C$ and O_2/N_2 observations. *Tellus* **51B**, 213–232.

Rintoul, S. R. and Bullister, J. L. 1999. A late winter hydrographic section from Tasmania to Antarctica. *Deep-Sea Res. I* **46**, 1417–1454.

Rintoul, S. R., Donguy, J. R. and Roemmich, D. H. 1997. Seasonal evolution of upper ocean thermal structure between Tasmania and Antarctica. *Deep-Sea Res. I* **44**, 1185–1202.

Roemmich, D. and Cornuelle, B. 1992. The subtropical mode water of the South Pacific Ocean. *J. Geophys. Res.* **22**, 1178–1187.

Roy, T., Rayner, P., Matear, R. and Francey, R. 2003. Southern hemisphere ocean CO_2 uptake: reconciling atmospheric and oceanic estimates. *Tellus* **55B**, 701–710.

Sabine, C. L. and Key, R. M. 1998. Controls on fCO_2 in the South Pacific. *Mar. Chem.* **60**, 95–110.

Sokolov, S. and Rintoul, S. R. 2002. Structure of Southern Ocean fronts at 140°E. *J. Mar. Syst* **37**, 151–184.

Takahashi, T., Feely, R. A., Weiss, R. F., Wanninkhof, R. H., Chipman, D. W. et al. 1997. Global air–sea flux of CO_2. *Proc. Natl. Acad. Sci., USA* **94**, 8292–8299.

Takahashi, T., Sutherland, S. C., Feely, R. A. and Cosca, C. E. 2003. Decadal variation of the surface water PCO_2 in the western and central equatorial Pacific. *Science* **302**, 852–856.

Takahashi, T., Sutherland, S. C., Sweeney, C., Poisson, A., Metzl, N. et al. 2002. Global sea–air CO_2 flux based on climatological surface ocean pCO_2, and seasonal biological and temperature effects. *Deep-Sea Res. II* **49**, 1601–1622.

Takahashi, T., Wanninkhof, R. H., Feely, R. A., Weiss, R. F., Chipman, D. W. et al. 1999. Net sea–air CO_2 flux over the global oceans: an improved estimate based on the sea–air pCO_2 difference. In: *Proceedings of the 2nd International Symposium, CO_2 in the Oceans*, Tsukuba, Japan, 9–15. CGER/NIES, Tsukaba.

Tans, P. P., Fung, I. Y. and Takahashi, T. 1990. Observational constrains on the global atmospheric CO_2 budget. *Science* **247**, 1431–1438.

Terazaki, M., Ogawa, H. and Tamaki, K. 2003. *Preliminary Report of the R/V Hakuho Maru Cruise KH-01-3. Southern Pacific and Southern Ocean. Studies on the Biological Production and Biogeochemical Cycles in the Central Southern Pacific and Southern Ocean and Geophysical Study of Australia-Antarctic Ridge*. Ocean Research Institute, University of Tokyo.

Tréguer, P. and Jacques, G. 1992. Dynamics of nutrients and phytoplankton, and fluxes of carbon, nitrogen and silicon in the Antarctic Ocean. *Polar Biol.* **12**, 149–162.

Yaremchuk, M., Bindoff, N. L., Schröter, J., Nechaev, D. and Rintoul, S. R. 2001. On the zonal and meridional circulation and ocean transports between Tasmania and Antarctica. *J. Geophys. Res.* **106**(C2), 2795–2814.